

## Evidence for the Influence of Interfacial Atomic Structure on Electrical Properties at the Epitaxial $\text{CaF}_2/\text{Si}(111)$ Interface

J. L. Batstone, Julia M. Phillips, and E. C. Hunke<sup>(a)</sup>

*AT&T Bell Laboratories, Murray Hill, New Jersey 07974*

(Received 30 November 1987)

The atomic structure at the epitaxial  $\text{CaF}_2/\text{Si}(111)$  interface has been determined by high-resolution electron microscopy. As-grown layers reveal only direct Ca-Si bonding at the interface, with eightfold coordinated Ca atoms. Fluorine is preferentially removed from the interface during a rapid thermal anneal leaving fivefold coordinated Ca atoms. Removal of F results in a dramatic improvement in the electrical properties of the interface. The measured interface state density is reduced from  $\gtrsim 10^{13} \text{ cm}^{-2}$  to  $\lesssim 10^{11} \text{ cm}^{-2}$ .

PACS numbers: 61.16.Di, 73.20.Hb

$\text{CaF}_2$  grows epitaxially on both  $\text{Si}(100)$  and  $(111)$ .<sup>1</sup> Technological interest in this system centers around its high-quality crystalline insulator-semiconductor interfaces and the possibilities of three-dimensional integration and dielectric isolation.  $\text{CaF}_2$  and Si have very similar cubic lattice structures, and a room-temperature misfit of 0.6%. The successful fabrication of metal-epitaxial insulator-semiconductor field-effect transistors<sup>2</sup> has shown that device quality is particularly sensitive interfacial perfection. Consequently, knowledge of the interfacial atomic structure, coupled with an understanding of how it affects the electrical properties of the interface, will make possible the optimization of device performance. From a more fundamental standpoint, the  $\text{CaF}_2/\text{Si}(111)$  interface offers an excellent opportunity to study bonding configurations and epitaxial relationships at the ionic-covalent interface. Photoemission data from this interface suggest that both Ca-Si and F-Si bonds are present.<sup>3,4</sup> While photoemission can give an indication of the electronic structure of an interface, it cannot be used to determine the geometry of the interface directly. The models arising from these studies must therefore be regarded as tentative<sup>4</sup> until corroborated by other techniques.

We present high-resolution electron microscopy (HREM) data of the  $\text{CaF}_2/\text{Si}(111)$  interface from both as-grown and rapidly thermally annealed (RTA) films. Comparison of these data with simulations of different bonding configurations and rigid shift measurements suggests that the interface in as-grown films consists of Ca-Si bonds, with the Ca atom eightfold coordinated. The coordination of the Ca atom changes to fivefold after RTA because of removal of F from the interface; the crystallinity of the interface is preserved. The loss of interfacial F results in a drop of several orders of magnitude in the interface state density.

$\text{CaF}_2$  was grown on  $\text{Si}(111)$  as described previously.<sup>5</sup> The epitaxial quality of  $\text{CaF}_2$  layers as measured by electron channeling improves considerably after RTA. RTA was performed in a commercially available flash-

lamp annealing system.<sup>6</sup> The interface structure was examined with use of HREM in both as-grown and RTA samples. Films were prepared in cross section by mechanical polishing and Ar ion milling. TEM examination was performed in JEOL model 4000EX operating at 200 kV to minimize radiolysis of the  $\text{CaF}_2$ .<sup>7</sup> The point-to-point resolution at 200 kV is 2.3 Å near Scherzer defocus, allowing the faithful resolution of the  $(111)$  and  $(200)$  planes in both Si and  $\text{CaF}_2$  in the  $\langle 110 \rangle$  projection. Reliable direct image interpretation is constrained by sample thickness and the resulting multiple elastic scattering effects (*Pendellösung*). Calculations of *Pendellösung* effects were performed with a multislice algorithm.<sup>8</sup> Multiple-scattering effects for thicknesses  $< 75$  Å at 200 kV in both Si and  $\text{CaF}_2$  in the  $\langle 110 \rangle$  projection do not affect the accuracy of rigid shift measurements.

Figure 1(a) shows a  $\langle 110 \rangle$ -projection lattice image of the as-grown  $\text{CaF}_2/\text{Si}(111)$  interface. The interface is atomically abrupt, as seen previously.<sup>9</sup> The epitaxial film has a type-B orientation where the film is rotated 180° with respect to the substrate normal. The interface is discommensurate<sup>10</sup> containing  $(a/6)\langle 112 \rangle$  misfit dislocation (not shown), associated with interfacial steps. This observation implies a unique interface bonding configuration. In the absence of  $(a/6)\langle 112 \rangle$  dislocations, a step would result in a change in coordination for the Ca atom. The quality of the TEM sample depends sensitively on preparation conditions. Amorphous pockets commonly observed at the interface<sup>9</sup> could be minimized by optimization of sample-preparation procedures.<sup>11</sup> Although point-defect damage can be induced by the electron beam, the planar spacings and symmetry of the crystal were preserved, such that the bonding arrangements could be inferred. Nevertheless, prolonged electron-beam irradiation resulted in radiolysis of the  $\text{CaF}_2$  and the subsequent destruction of the interfacial crystallinity. The image in Fig. 1(a) was recorded close to Scherzer defocus ( $-600$  Å) such that atom positions appear black. The white dots correspond to minima in

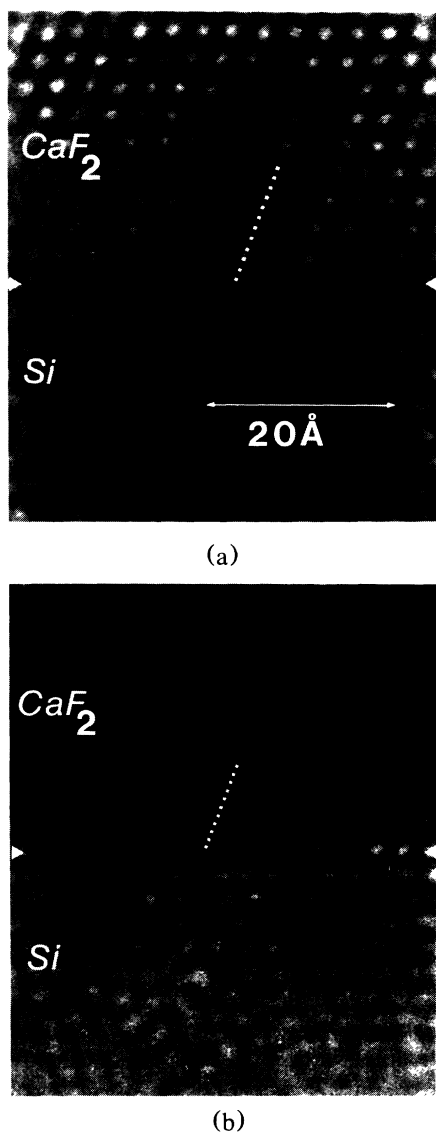


FIG. 1. Axial  $\langle 110 \rangle$  bright-field images of the  $\text{CaF}_2/\text{Si}(111)$  interface: (a) as grown and (b) after RTA. The interface crystallinity is preserved even after a very high-temperature anneal.

the projected crystal potential, i.e., tunnels in the crystal lattice. The sample thickness was chosen (by examination of *Pendellösung*) to allow simple direct image interpretation. However, the image does not resolve individual atom positions directly, because of the unresolved (400) spacing (1.35 Å). Consequently, the interfacial atomic structure must be inferred from rigid shift measurements and image simulations.

Figure 1(b) shows a  $\langle 110 \rangle$  HREM image of the  $\text{CaF}_2/\text{Si}(111)$  interface after RTA. The crystallinity of the interface is preserved. Inspection of the interfaces in Figs. 1(a) and 1(b) suggests that the interfacial structure has not changed significantly as a result of RTA.

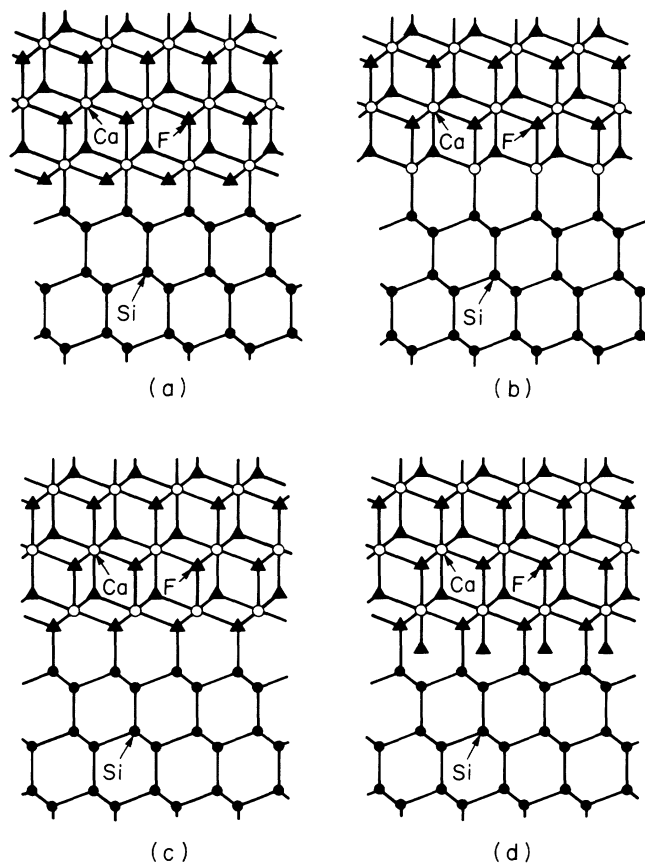


FIG. 2. Model structures for the  $\text{CaF}_2/\text{Si}(111)$  interface: (a) Ca-Si interface bonds, eightfold-coordinated Ca; (b) Ca-Si interface bonds, fivefold-coordinated Ca; (c) F-Si interface bonds, sevenfold-coordinated Ca; and (d) F-Si interface bonds, eightfold-coordinated Ca.

In undertaking the analysis of the structure at the epitaxial  $\text{CaF}_2/\text{Si}(111)$  interface, it is instructive to note the interfacial atomic structure at widely studied epitaxial metal silicide-silicon interfaces. Like  $\text{CaF}_2$ ,  $\text{NiSi}_2$ , and  $\text{CoSi}_2$  both have the cubic fluorite structure and grow epitaxially on  $\text{Si}(111)$ . In the bulk crystal, each metal atom is surrounded by eight bonds and is described as eightfold coordinated. HREM has revealed that Ni atoms are sevenfold coordinated at the  $\text{NiSi}_2/\text{Si}(111)$  interface<sup>12</sup> with each Ni atom associated with one dangling bond. The  $\text{NiSi}_2$  bonds to the substrate via its Si atoms. In contrast, Co atoms show apparent fivefold coordination at the  $\text{CoSi}_2/\text{Si}(111)$  interface<sup>13,14</sup> with the  $\text{CoSi}_2$  bonding to the substrate via its metal atoms. Analogous bonding configurations may be postulated to exist at the  $\text{CaF}_2/\text{Si}(111)$  interface with the additional possibility of either Ca-Si or F-Si interface bonds.

Figure 2 shows four possible bonding configurations at the  $\text{CaF}_2/\text{Si}(111)$  interface. All four models have been proposed with the assumption that silicon *always* main-

tains its bulk tetrahedral coordination.<sup>12</sup> In Fig. 2(a), the interface consists of Ca–Si bonds with the Ca atom maintaining its bulk eightfold coordination. Each interfacial F atom has two dangling bonds. Ca–Si interface bonds can also be obtained with the Ca atom fivefold coordinated if the layer of F atoms present at the interface is removed as illustrated in Fig. 2(b). This bonding configuration has been proposed for the  $\text{CoSi}_2/\text{Si}(111)$  interface.<sup>13,14</sup> The relative displacements of the  $\text{CaF}_2$  and Si lattices are identical for these two models. The  $\text{CaF}_2$  molecule can also bond to the substrate via its F atoms. Figure 2(c) shows a sevenfold-coordinated Ca atom with F–Si interface bonds. The unlikely eightfold-coordinated Ca atom with F–Si bonds is shown in Fig. 2(d) where each F atom has three missing bonds. Figures 2(c) and 2(d) have identical lattice displacements, and are distinguishable from Figs. 2(a) and 2(b). The rigid shifts between the  $\text{CaF}_2$  and Si lattices can be determined by our treating the twin boundary at the interface as a coherent coincidence boundary.<sup>15</sup> Although the boundary occurs between two different crystal structures, the symmetry of the two crystals is identical in the  $\langle 110 \rangle$  projection. As a result, the rigid shifts may be defined relative to a coincidence site lattice.

It is possible to distinguish between the eightfold and fivefold-coordinated models on one hand and the sevenfold-coordinated model on the other by measurement of the rigid shifts; it is not necessary to resort to simulations. Analysis of the models shown in Fig. 2 confirms the expected small shift of the (111) planes at the interface in the [112] direction for both the eightfold and fivefold-coordinated models, which is absent in the sevenfold model.<sup>13</sup> This shift is visible in the HREM image in Fig. 1(a); the white dot at the interface is shifted with respect to the dotted line. Examination of Fig. 1(a) also reveals an  $\approx 8\%$  contraction of the (111) planar spacing at the interface. This agrees well with that observed in simulated images of the eightfold-coordinated interface in Fig. 2(a).<sup>16</sup> A sevenfold-coordinated interface [Fig. 2(c)] would result in an expansion of the planar spacings, contrary to our observations.

In Fig. 1(b), the planar shifts across the  $\text{CaF}_2/\text{Si}(111)$  interface after RTA again suggest eightfold or fivefold coordination with Ca–Si bonding at the interface. Distinction between the fivefold and eightfold models relies on very subtle changes in contrast which were indistinguishable in experimental images. However, analysis of the planar spacings near the interface reveals a 15%–20% contraction, in contrast to the smaller  $\approx 8\%$  contraction seen in as-grown samples. This extra contraction can be explained by the assumption that the interface relaxes to a fivefold-coordinated interface [Fig. 2(b)]. Removal of a layer of interfacial F atoms from the eightfold-coordinated interface should lead to contraction of the Si–Ca bonds in light of the more covalent bonding (and hence shorter bond length) between

these two species arising from the lower coordination number of the Ca.

The loss of F from the  $\text{CaF}_2/\text{Si}(111)$  interface upon annealing is consistent with previous observations.  $\text{CaF}_2$  will dissociate during high-temperature annealing.<sup>17</sup> In addition, F is preferentially removed from the interface during RTA if oxygen is present in the annealing ambient.<sup>7</sup> Some F loss probably occurs even if the anneal is performed in an inert atmosphere. The HREM observation of the reduction of an eightfold-coordinated interface to a fivefold-coordinated one is very easy to visualize, since it does not involve any atomic rearrangement, but only the removal of partially coordinated F.

It is enlightening to correlate the change in the interfacial structure as a function of an RTA with electrical measurements performed on these  $\text{CaF}_2$  films on Si(111). As discussed in Ref. 3, the last layer of F at the eightfold-coordinated as-grown interface has only two bonds to Ca, instead of the usual four found in bulk  $\text{CaF}_2$ . In addition, the Ca–Si bond is considerably more covalent than are the highly ionic Ca–F bonds. The interfacial F must find an electron from elsewhere than the Ca to fill its outer orbital. This gives a layer of net negative charge at the interface, which has dramatic consequences for the electrical properties. If the F layer at the interface is complete, the density of  $\text{F}^-$  ions is  $\approx 8 \times 10^{14} \text{ cm}^{-2}$ . For layers grown on *p*-type Si, the layer of negative charge is attractive to the majority-carrier holes, resulting in an interface that is in accumulation for all voltages less than the insulator breakdown. This interface cannot be inverted.<sup>18</sup> The observed Fermi-level pinning at the interface implies an interface state density  $\gtrsim 10^{13} \text{ cm}^{-2}$ . For layers grown on *n*-type Si,<sup>19</sup> the layer of negative charge repels the majority-carrier electrons and attracts the minority carriers, making inversion easy. There is a region between inversion and accumulation where the negative charge of the  $\text{F}^-$  ions is just balanced by minority carriers in the Si at the interface. This is a stable configuration which persists for a wide range of voltages, resulting in a plateau in the high-frequency *C-V* characteristics. Accumulation at this interface requires very high fields, generally near or above the breakdown field of the insulator. All of these features have been observed. The trap density at this interface has been determined to be  $\approx 3 \times 10^{12} \text{ cm}^{-2}$ . This value is lower than predicted, possibly because the sample preparation employed in these experiments may have led to some F loss at the interface, which would result in a smaller net charge at the interface.

After RTA, the interfacial F has been eliminated. All remaining F has its bulklike coordination. The interfacial Ca is fivefold coordinated. Four of its bonds are with F and are highly ionic. The fifth bond is with Si and is only slightly ionic. As hypothesized in Ref. 3, this results in a stable, neutral interface which exhibits reasonable electrical characteristics, and dramatically

lowered interface state densities ( $\lesssim 10^{11} \text{ cm}^{-2}$ ).<sup>18</sup>

Both our HREM results and recent photoemission data<sup>3,4</sup> reveal a large number of Ca–Si bonds. The upward shift in energy of the F 1s Auger peak in Fig. 1 of Ref. 4 indicates that F at the interface is less negatively charged than in bulk CaF<sub>2</sub>. This finding is consistent with our observation of twofold-coordinated interfacial F in as-grown samples.

In summary, we have used HREM to determine directly the interface bonding configuration at epitaxial CaF<sub>2</sub>/Si(111) interfaces. Ca–Si bonds are formed at the interface. No evidence for F–Si interface bonds is observed. We propose that the as-grown interface contains eightfold-coordinated Ca atoms. Measurements of the planar spacings across the interface suggest that F is removed from the interface during RTA, leaving a fivefold-coordinated Ca atom. These findings provide a natural explanation for the dramatic improvement seen in the electrical properties of the CaF<sub>2</sub>/Si(111) interface after RTA.

We are grateful to J. M. Givson for assistance with image simulations, to F. Sette for enlightening comments on the photoemission experiments, and to R. People for useful discussion on the electrical properties of the CaF<sub>2</sub>/Si(111) interface. D. Bahnck prepared the samples for HREM examination.

---

<sup>(a)</sup>Permanent address: Memphis State University, Memphis, TN 38152.

<sup>1</sup>See, for example, J. M. Phillips, *Mater. Res. Soc. Symp. Proc.* **71**, 97 (1986); H. Ishiwara, T. Asano, H. C. Lee, Y. Kuriyama, K. Seki, and S. Furukawa, *Mater. Res. Soc. Symp. Proc.* **67**, 105 (1986); L. J. Schowalter and R. W. Fathauer, *J. Vac. Sci. Technol. A* **4**, 1026 (1986).

<sup>2</sup>T. P. Smith, III, J. M. Phillips, W. M. Augustyniak, and P. J. Stiles, *Appl. Phys. Lett.* **45**, 907 (1984).

<sup>3</sup>M. A. Olmstead, R. I. G. Uhrberg, R. D. Bringans, and R. Z. Bachrach, *Phys. Rev. B* **35**, 7526 (1987).

<sup>4</sup>F. J. Himpsel, U. O. Karlsson, J. F. Morar, D. Reiger, and J. A. Yarmoff, *Phys. Rev. Lett.* **56**, 1497 (1986), and *Mater. Res. Soc. Symp. Proc.* **94**, 181 (1987).

<sup>5</sup>J. M. Phillips, L. N. Pfeiffer, D. C. Joy, T. P. Smith, III, J. M. Gibson, W. M. Augustyniak, and K. W. West, *J. Electrochem. Soc.* **133**, 224 (1986).

<sup>6</sup>L. N. Pfeiffer, J. M. Phillips, T. P. Smith, III, W. M. Augustyniak, and K. W. West, *Appl. Phys. Lett.* **46**, 947 (1985).

<sup>7</sup>R. W. Fathauer, L. J. Schowalter, N. Lewis, and E. L. Hall, *Mater. Res. Soc. Symp. Proc.* **54**, 313 (1986).

<sup>8</sup>J. M. Cowley and A. F. Moodie, *Acta Crystallogr.* **10**, 609 (1957).

<sup>9</sup>F. A. Ponce, G. B. Anderson, M. A. O'Keefe, and L. J. Schowalter, *J. Vac. Sci. Technol. B* **4**, 1121 (1986); F. A. Ponce, M. A. O'Keefe, and G. B. Anderson, presented at Spring Meeting of the Materials Research Society, Palo Alto, California, April 1986 (unpublished).

<sup>10</sup>J. M. Gibson and J. M. Phillips, *Appl. Phys. Lett.* **43**, 828 (1983).

<sup>11</sup>D. Bahnck, J. L. Batstone, and J. M. Phillips, to be published.

<sup>12</sup>D. Cherns, G. R. Anstis, J. L. Hutchison, and J. C. H. Spence, *Philos. Mag. A* **46**, 849 (1982).

<sup>13</sup>J. M. Gibson, J. C. Bean, J. M. Poate, and R. T. Tung, *Appl. Phys. Lett.* **9**, 818 (1982).

<sup>14</sup>J. Zegenhagen, K. G. Huang, B. D. Hunt, and L. J. Schowalter, *Appl. Phys. Lett.* **51**, 1176 (1987).

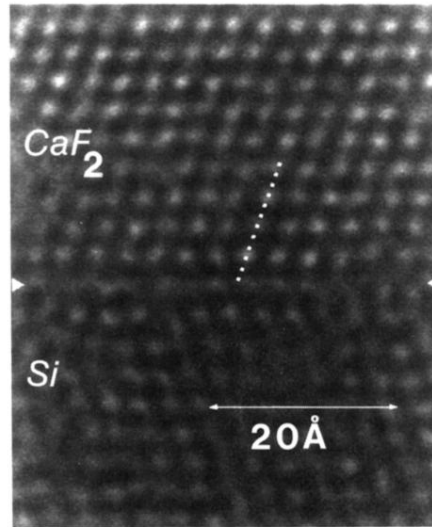
<sup>15</sup>A description of the coincidence site lattice can be found in A. G. Guy, *Introduction to Materials Science* (McGraw-Hill, New York, 1971).

<sup>16</sup>J. L. Batstone, J. M. Phillips, and E. C. Hunke, *Mater. Res. Soc. Symp. Proc.* (to be published). The best fit to the data, the simulations shown in Fig. 3 of this reference, were calculated at 200 kV for a thickness of 62 Å and a defocus of –650 Å.

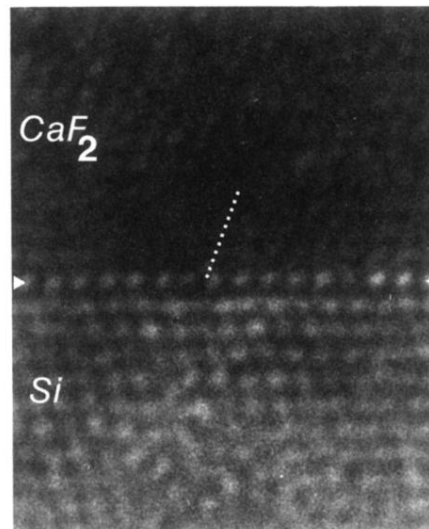
<sup>17</sup>M. A. Olmstead, R. I. G. Uhrberg, R. D. Bringans, and R. Z. Bachrach, *J. Vac. Sci. Technol. B* **4**, 1123 (1986).

<sup>18</sup>J. M. Phillips, M. L. Manger, L. N. Pfeiffer, D. C. Joy, T. P. Smith, III, W. M. Augustyniak, and K. W. West, *Mater. Res. Soc. Symp. Proc.* **53**, 155 (1986).

<sup>19</sup>L. J. Schowalter and R. W. Fathauer, in *Proceedings of the First International Symposium on Si Molecular Beam Epitaxy*, edited by J. C. Bean (Electrochemical Society, Pennington, NJ, 1985), Vol. 85-7, p. 311.



(a)



(b)

FIG. 1. Axial  $\langle 110 \rangle$  bright-field images of the CaF<sub>2</sub>/Si(111) interface: (a) as grown and (b) after RTA. The interface crystallinity is preserved even after a very high-temperature anneal.